Journal of Physics: Conference Series **484** (2014) 012012 doi:10.1088/1742-6596/484/1/012012

Spherical gravitational wave detectors: MiniGRAIL and Mario Schenberg

C F Da Silva Costa and O D Aguiar

USP and INPE, São Paulo, Brazil

E-mail: filipe.dasilva@usp.br, odylio.aguiar@inpe.br

Abstract. Spherical gravitational wave detectors allow the analysis of multiple independent channels and, therefore, are able to determine gravitational wave directions and polarizations. There are two spherical detectors being developed now: MiniGRAIL (Netherlands) and Mario Schenberg (Brazil). Both share the same principle of detection and main features. They have done commissioning runs and shown progress in their development. We have presented here the status of Mario Schenberg. Its transducers have been redesigned for sensitivity improvements. While an offline analysis was already developed for MiniGRAIL, we have investigated a low latency data analysis technique for Mario Schenberg. Both analysis are based on directional detection.

1. Introduction

Two spherical resonant mass detectors are being developed: MiniGRAIL (Netherlands) [1] and Mario Schenberg (Brazil) [2, 3] (see Section 2). Their last commissioning runs were respectively, in autumn 2010 and in 2008. Similar to bars, surface oscillations are measured in order to look for gravitational waves signatures. Unlike bars that only monitor one mode, the spherical shape allows an isotropic and a multichannel analysis of signals. Actually, gravitational waves (GW) couple to the five quadrupolar modes of the sphere (see Section 3). The spherical shape also provides a better effective mass than a bar [4]. Despite their narrow band, spherical gravitational detectors are a low cost solution that could play a significant role in gravitational astrophysics, since one detector can determine alone the direction of a GW source.

An offline analysis has been already developed for MiniGRAIL (see Section 4), and a low latency analysis using similar principle as the offline analysis is under development (see Section 5). These analysis techniques could be applied to both detectors with minor changes.

2. Experiment description

Both spheres of MiniGRAIL and Mario Schenberg are made of CuAl (6%) alloy, which provides a high mechanical $Q \sim 10^7$. Their respective masses and diameters are 1400 kg/68 cm, and 1150 kg/65 cm, which give resonant frequencies $f_0 \sim 3$ kHz. External vibrations (seismic noise) are attenuated by a dumping system composed of hanging masses: by ~ 350 dB@3 kHz (MiniGRAIL), and ~ 400 dB@3.2 kHz (Mario Schenberg). Both antennas aim to operate at temperature of ~ 50 mK in order to reduce thermal noise.

The mechanical vibrations of the sphere are converted into electromagnetic (EM) signals by six transducers. MiniGRAIL uses capacitive transducers amplified by 2-stage SQUID systems

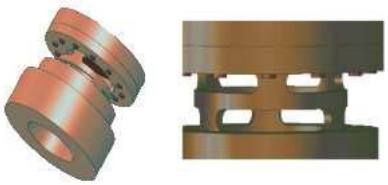

Figure 1. Scheme of the 5th transducer generation. The lower ring (left) is introduced in the sphere holes. The middle part works as a spring, which will be tuned to the sphere resonant frequency at low temperature. The upper part contains the electromagnetic resonant cavity, which is closed by a 50 μm membrane thick. This transducer is ~ 30 mm diameter [7].

(dc-SQUIDs from Quantum Design) [5]. Instead of passive transducers, Mario Schenberg is the first spherical detector to use parametric transducers with resonant cavities of klystron type [6] (see Figure 1). These transducers could allow quantum squeezing. The resonant cavity is pumped with a microwave signal of 10 GHz, which is modulated by the oscillations of the transducer ($df/dx \sim 0.5\,\mathrm{GHz}/\mu\mathrm{m}$). These modulations are thus, analyzed. The contact between transducers and the sphere is done by thermal contraction of the sphere. Bodies and membranes of the transducers are both made of niobium, which minimizes the differential thermal contraction between parts after cooling down. Since their first design [2], a large effort has been done to increase the transducer sensitivity. Instead of microstrip antennas (commonly used), a new technique has been developed to couple directly the EM probe to the cavity and moreover from outside of it. In this way, it avoids thermic and seismic noise transmission. A commissioning run to test the new technologies is planned by the end of 2012.

2.1. Data acquisition system

We have written our own software to control and manage the acquisition (ADC, GPS, VXI-PC cards). We have tested the synchronization between the GPS Pulse Per Second (PPS) and the data acquisition. For a given sampling frequency f_s, we get a timing error of $1/f_\mathrm{s}$ [8]. Scintillators are also being installed and calibrated to veto high energetic astroparticle showers, which could interact with the sphere.

3. Mode channels

GW couple with the five quadrupolar modes of the sphere [9, 10]. These quadrupolar modes have frequencies around 2980 Hz (MiniGRAIL) within a bandwidth of ~ 230 Hz, and 3200 Hz (Mario Schenberg) within a bandwidth of ~ 80 Hz. In order to monitor these normal modes, six transducers are disposed following the TIGA configuration [11, 12]. Transducers signals are converted into the quadrupolar components h_m (m mode channels) by:

$$h_m(\omega) = T_{mk}(\omega)V_k(\omega), \quad m = 1, ..., 5 \text{ and } k = 1, ..., 6, \tag{1}$$

where T_{mk} is the system transfer function (calibrated), and V_k are the tensions provided by the k transducers. After solving analytically T_{mk} using the TIGA configuration, we have determined the GW tensor h_{ij}, which are directly related to the quadrupolar mode h_m by:

$$h_{ij} = h_m Y^m_{ij}, \tag{2}$$

where Y^m_{ij} is a quadrupolar tensor basis (i.e., traceless and symmetric tensors) used to express the spherical harmonic Y^m_2 [9, 13]. This basis is explicitly defined in [14].

Thus, these five quadrupolar modes provide the complete information about the gravitational waves: direction and polarization.

4. Offline analysis

A complete data analysis pipeline has been developed for MiniGRAIL [15, 16]. It uses the Coherent Waveburst for the Sphere (CWS), an adaptation of the Klimenko's Waveburst [17], to generate lists of triggers. This method presents the advantage of not depending on the signal waveform and direction as the Matched Filter (MF) technique does.

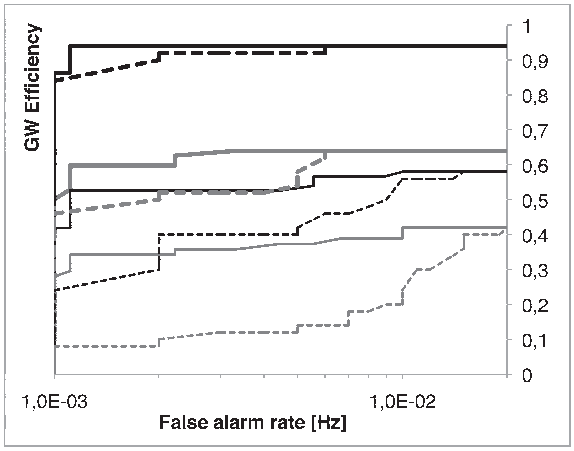

Figure 2. ROC: Detection efficiency vs. false alarm rate for signal injections (Sine-Gaussian) of increasing amplitude: $h_{rss} = \{3, 5, 7, 10\} \times 10^{-21}\mathrm{Hz}^{-1/2}$ (respectively, lines of increasing thickness). Broken and solid lines refer to the angular distance respectively between the CWS and the determinant method, and between CWS and MF methods.

The triggers are vetoed by two independent direction reconstructions: A likelihood method and an algebraic method based on the transverse traceless properties of the GW matrix. Using a Receiver Operation Characteristic (ROC), we select a threshold of 0.2 radians between the two directions. All triggers with a higher difference are discarded. After the CWS, we have used a linear MF that takes into account noise correlation among the five channels and the noise evolution. The MF maximizes the SNR and thus, compared to the CWS, it increases the time precision by one order of magnitude, giving an error of 10 ms. The signal amplitude is estimated with an accuracy of 10%. The MF allows a third direction reconstruction ((θ or ϕ) = 15 - 60 mrad) reducing again by a factor ~ 3 the false alarm rate. In Figure 2, we have shown the ROC of GW efficiency to false alarm rate. It is obtained by varying the maximum allowed distance between the direction reconstruction methods. We can exclude 90% of non-GW signals.

5. Low latency detection

GW triggers of high SNR could be confronted with other event messengers like neutrinos, gamma rays, and other signals, if a fast identification of these triggers is provided. We have been developing and testing a low latency analysis pipeline. In order to reduce the computational time, the transfer function is computed before data acquisition and it is stored on disk. It relies on an analytic solution and the parameters of the present status of the detector.

Triggers are defined by a SNR threshold. The SNR is calculated considering previous noise levels, but for simplification, the SNR calculation does not take into account the correlations between channels. As the detector is narrow band, we have used a pass band filter, which is continuously adjusted to the best strain sensitivity zone.

Generated triggers are vetoed primarily by checking for glitches or cosmic rays. To confirm that our trigger could be a possible event, we have checked if its energy is deposited following a spherical quadrupolar pattern. An indirect way to test this deposition is, thus, to reconstruct the GW arrival direction for each bin in the frequency window. We have constructed two histograms, one for each direction angle. A signal having a quadrupolar distribution generates a Gaussian distribution around the direction with a low variance. On the other hand, noise produces a false direction with a large variance. Evidently, this also depends on the SNR level. In Figure 3, we

have shown variances for different signal injections amplitudes. Like the offline analysis, a follow up MF is being tested.

In this method, the computational time is maintained below the acquisition time. For example, on a 2.4 GHz processor, it needs ~ 2 s to process for 4 s of data and ~ 9 s for 32 s of data ($f_s = 16384$ Hz). The most time consuming parts are FFT transformations.

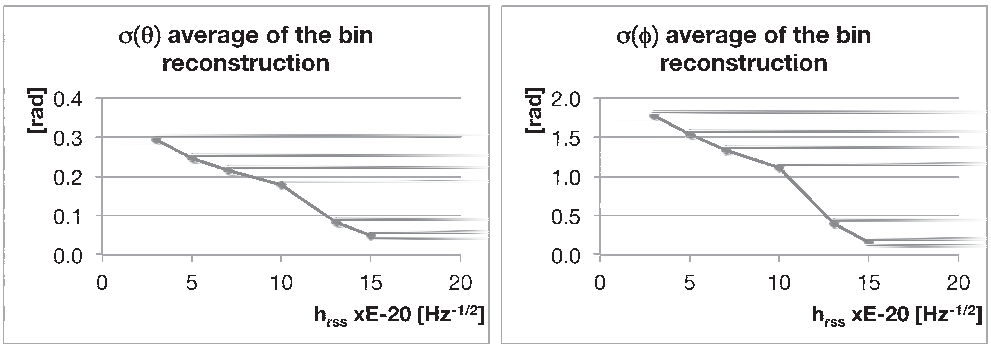

Figure 3. We inject Sine-Gaussian signals covering the entire sensitive frequency band with direction: $\theta = 0.62$ and $\phi = -2.60$ (Euler angles), and six different amplitudes h_{rss}. For each amplitude, we do an average over 25 injections. Here, we have shown the direction re-construction variances for each signal amplitude. Signal injections are done in our simulator to include signal deformations due to mechanical and electrical attenuations.

6. Conclusion

This low latency method will be able to provide fast direction re-construction with a good confidence for high SNRs. In order to increase the GW detection efficiency of the offline analysis, we have been also investigating the use of Bayesian method for un-modelled bursts as described in [18]. Resonant spheres are a promising technique, and obtaining a better strain sensitivity is purely a technological problem. Another transducer technology for monitoring more than the fundamental modes will turn spherical detectors into large band detectors.

Acknowledgements

This work has been supported by FAPESP (under grants No. 2010/09101-6 and project grants 2006/56041-3). To C A Costa and S Foffa for their help.

References

[1] de Waard A, Bassan M, Benzaim Y, Fafone V *et al* 2006 *Class. Quant. Grav.* **23** S79
[2] Aguiar O D, Andrade L A, Barroso J J *et al* 2006 *Class. Quant. Grav.* **23** S239
[3] Costa C A *et al* 2008 *Class. Quant. Grav.* **25** 184002
[4] Lenzi C H, Magalhães N S *et al* 2008 *Phys. Rev. D* **78** 062005
[5] Gottardi L 2007 *Phys. Rev. D* **75** 022002
[6] Pimentel G L, Aguiar O D, Barroso J J and Tobar M E 2008 *J. Phys. Conf. Ser.* **122** ed Science I
[7] Aguiar O D *et al* 2012 *J. Phys. Conf. Ser.* **363** 012003
[8] Da Silva Costa C F *et al* 2012 *Gravitational wave antenna Mario Schenberg: Data acquisition system manual sid.inpe.br/mtc-m19/2012/04.17.15.03 INPE, Brazil*
[9] Zhou C Z and Michelson P F 1995 *Phys. Rev. D* **51**(6) 2517
[10] Costa C A, Aguiar O D and Magalhães N S 2003 [gr-qc/0312035]
[11] Johnson W W and Merkowitz S M 1993 *Phys. Rev. Lett.* **70** 2367
[12] Merkowitz S M and Johnson W W 1997 *Phys. Rev. D* **56** 7513
[13] Maggiore M 2008 *Gravitational Waves* **1** *Theory and Experiments* (Oxford University Press)

[14] Da Silva Costa C F 2010 *Data Analysis Pipeline for the Spherical Gravitational Wave Antenna MiniGRAIL* thesis nb. 4210 *Faculte des sciences de l'Universite de Geneve*
[15] Foffa S and Sturani R 2009 *Class. Quant. Grav.* **26** 105013
[16] Da Silva Costa C F, Foffa S and Sturani R 2009 *Class. Quant. Grav.* **26** 204019
[17] Klimenko S and Mitselmakher G 2004 *Class. Quant. Grav.* **21** S1819
[18] Searle A C, Sutton P J and Tinto M 2009 *Class. Quant. Grav.* **26** 155017